Proceedings Paper:

Al Zamzami, I., Razavi, S.M.J., Berto, F. et al. (1 more author) (2020) The Critical Distance Method to estimate the fatigue strength of notched additively manufactured titanium alloys. In: Iacoviello, F., Sedmak, A., Marsavina, L., Blackman, B., Ferro, G.A., Shlyannikov, V., Ståhle, P., Zhang, Z., Moreira, P.M.G.P., Božic, Ž. and Banks-Sills, L., (eds.) Procedia Structural Integrity. 1st Virtual European Conference on Fracture - VECF1, 29 Jun - 01 Jul 2020, Virtual conference. Elsevier , pp. 994-1001.

https://doi.org/10.1016/j.prostr.2020.11.114

Available online at www.sciencedirect.com

ScienceDirect

Procedia Structural Integrity 28 (2020) 994–1001

Structural Integrity Procedia

www.elsevier.com/locate/procedia

1st Virtual European Conference on Fracture

The Critical Distance Method to estimate the fatigue strength of notched additively manufactured titanium alloys

I. Al Zamzami[a], S.M.J. Razavi[b], F. Berto[b], L. Susmel[a,*]

[a]Department of Civil and Structural Engineering, The University of Sheffield, Mappin Street, Sheffield S1 3JD, United Kingdom
[b]Norwegian University of Science and Technology, NO-7491 Trondheim, Norway

Abstract

The present investigation deals with the problem of performing the fatigue assessment of notched components made of 3D-printed titanium alloy Ti6Al4V when it is used in the as-manufactured condition. The notch fatigue strength of this additively manufactured metallic material was investigated by testing under axial loading a large number of specimens containing geometrical features of different sharpness. This experimental programme was designed to investigate also the effect of non-zero mean stresses, so that the experimental results were generated under a load ratio not only equal to -1, but also equal to 0.1. Being supported by the experimental evidence, the hypothesis was formed that the mechanical response of the 3D-printed titanium alloy being investigated could be modelled effectively by treating it as a material that is linear-elastic, homogenous and isotropic. This simplifying hypothesis allowed the Theory of Critical Distances to be employed also to assess the notch fatigue strength of 3D-printed titanium alloy Ti6Al4V weakened by geometrical features of different kind. The validation exercise based on the experimental results being generated demonstrates that this theory is highly accurate, with its use leading to predictions falling mainly within the scatter bands associated with the fatigue curves used for calibration. This level of accuracy is certainly satisfactory especially because the Theory of Critical Distances can be employed in situations of engineering relevance by making use of the results obtained by solving standard linear-elastic Finite Element models.

Keywords: Fatigue; notch; Theory of Critical Distances; additive manufacturing; titanium alloy Ti6Al4V

*Corresponding author. Tel.: +44 (0) 114 222 5073; fax: +44 (0) 114 222 5700.
E-mail address: l.susmel@sheffield.ac.uk

10.1016/j.prostr.2020.11.114

1. Introduction

Metals can be additively manufactured (AM) by making use of very fine metal powders or wires that are melted by employing either a laser or an electron beam. Compared to the large variety of metals that can be fabricated using conventional technologies, there is a limited choice of metallic materials that can be additively manufactured effectively. Common metals suitable for additive manufacturing (AM) include Ti-based and Ni-based alloys, various stainless steel grades and specific aluminium alloys.

Amongst the different AM technologies available in the market, the Direct Metal Laser Sintering (DMLS) process is certainly the most commonly adopted technological solution, with this holding particularly true in the biomedical and aerospace engineering field (Chan et al., 2013; Herzog et al., 2016).

In this manufacturing context, due to its relatively high mechanical properties and low density (i.e., high strength-to-weight ratio), titanium alloy Ti6A14V represents the most interesting choice for those applications where the use of light components is required (Qui et al., 2015). However, much experimental evidence demonstrates that components of AM Ti6A14V display an appropriate mechanical behaviour provided that they undergo *ad hoc* post-manufacturing processes (such as, for instance, heat-treatments). While these post-manufacturing processes certainly improve the mechanical response (and, in particular, the fatigue performance) of AM titanium alloys, they inevitably increase the overall fabrication costs.

One of the key features of AM is that objects having complex forms can be fabricated by reaching a very high level of accuracy in terms of both shape and dimensions.

From a structural integrity view point, the fact that 3D-printed components can contain very complex geometrical features results in localised stress concentration phenomena, with stress raisers reducing markedly the overall strength of the components themselves (Razavi et al., 2020). Accordingly, accurate and simple design techniques are required in order to perform the static assessment of 3D-printed materials accurately.

In this scenario, the aim of the research work summarised in this paper is investigating whether the linear-elastic Theory of Critical Distances (TCD) is successful in assessing the strength of 3D-printed notched Ti6A14V subjected to fatigue loading.

Nomenclature

k	negative inverse slope
K_t	net stress concentration factor
L_M	critical distance in the medium-cycle fatigue regime
N_f	number of cycles to failure
N_0	reference number of cycles to failure ($N_0=2\cdot10^6$ cycles to failure)
Oxyz	local system of coordinates
P_S	probability of survival
r_n	notch root radius
R	load ratio ($R=\sigma_{min}/\sigma_{max}$)
T_σ	scatter ratio of the endurance limit for 90% and 10% probabilities of survival
w_g	gross width
w_n	net width
θ, r	polar system of coordinates
$\Delta\sigma_{eff}$	range of the effective stress
$\Delta\sigma_{nom}$	range of the nominal net stress
$\Delta\sigma_0$	range of the plain endurance limit at N_0 cycles to failure for P_S=50%
$\Delta\sigma_{0n}$	range of the nominal net endurance limit at N_0 cycles to failure for P_S=50%
$\Delta\sigma_y$	range of the local linear-elastic stress parallel to axis y

2. Fundamentals of the Theory of Critical Distances

In its essence, the TCD postulates that the fatigue strength of notched engineering materials can be assessed via a specific critical distance-based effective stress, $\Delta\sigma_{eff}$, that is calculated by post-processing the entire linear-elastic stress field in the vicinity of the stress raiser under investigation (Taylor, 2007; Susmel, 2009).

The formalisations of the TCD proposed by Neuber (1958) and Peterson (1959) were originally devised to perform the fatigue assessment in the high-cycle fatigue regime. Nearly 50 years later, Susmel and Taylor (2007) reformulated the TCD to make it suitable for estimating fatigue damage also in the finite lifetime regime. This improved version of the TCD was formulated by taking as a starting point the hypothesis that the critical distance parameter needed to determine the required effective stress decreases as the number of cycles to failure increases, i.e.:

$$L_M(N_f) = A \cdot N_f^B \tag{1}$$

In the above definition (1), A and B are material constants that can be determined by running a series of suitable fatigue experiments. It is worth recalling here that, for a given material, constants A and B are seen to vary with the load ratio. In contrast, for a given material, their values do not change as profile and sharpness of the notch being designed change. The procedure to be followed to determine constants A and B in power law (1) will be reviewed in detail at the end of the present section.

As soon as the L_M vs. N_f relationship is known from the experiments, the TCD can be used in different forms, where its alternative versions can directly be derived by simply changing size and shape of the integration domain used to calculate the effective stress.

When the TCD is applied in the form of the Point Method (Tanaka, 1987; Taylor, 1999) the range of the effective stress is determined as follows (see Figs 1a and 1b):

$$\Delta\sigma_{eff} = \Delta\sigma_y\left(\theta = 0°, r = \frac{L(N_f)}{2}\right) \tag{2}$$

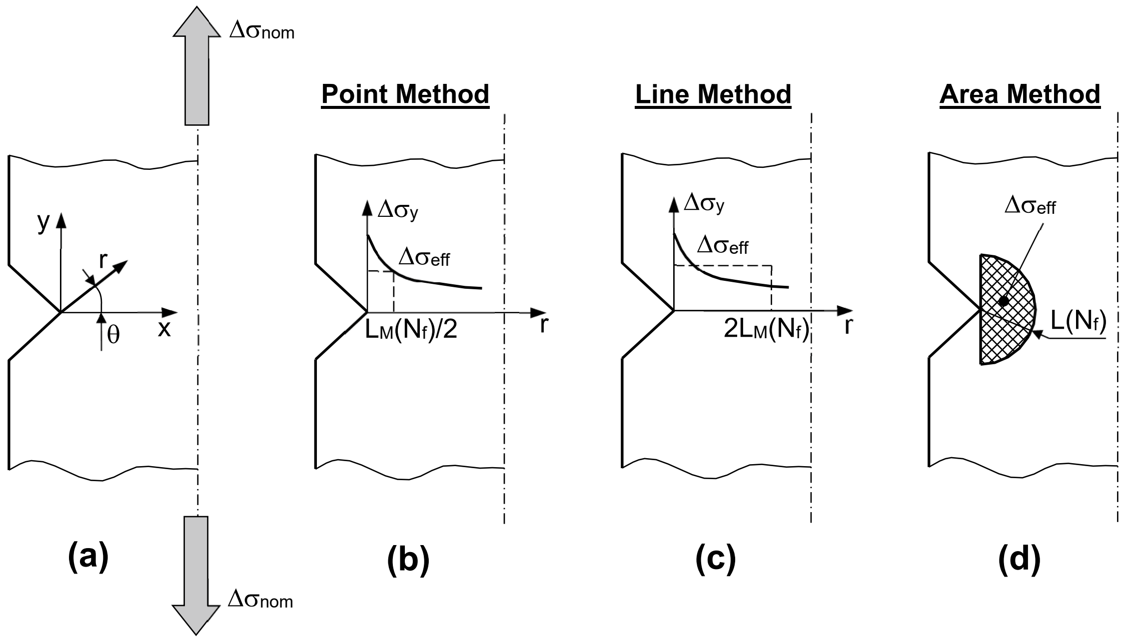

Fig. 1. Notched component subjected to fatigue loading (a); the TCD applied in the form of the Point (b), Line (c) and Area Method (d).

Alternatively, according to the Line Method (Taylor, 1999), the effective stress can also be determined by averaging the linear-elastic stress, $\Delta\sigma_y$, along a line over a distance equal to $2L_M(N_f)$, i.e. (Fig. 1c):

$$\Delta\sigma_{eff} = \frac{1}{2\cdot L_M(N_f)}\int_0^{2\cdot L_M(N_f)} \Delta\sigma_y(\theta = 0°, r)\cdot dr \tag{3}$$

Finally, the range of the effective stress can also be calculated by averaging the 1st principal stress range over a semicircle with radius equal to $L_M(N_f)$ and centred at the notch apex (Sheppard, 1991; Bellett et al. 2005). In other words, $\Delta\sigma_{eff}$ determined according to the so-called Area Method takes on the following value (Fig. 1d):

$$\Delta\sigma_{eff} = \frac{4}{\pi L_M^2(N_f)}\int_0^{\frac{\pi}{2}}\int_0^{L_M(N_f)} \Delta\sigma_1(\theta, r)\cdot r\cdot dr\cdot d\theta \tag{4}$$

Having determined $\Delta\sigma_{eff}$ according to one of the strategies reviewed above, the number of cycles to failure can then be estimated directly from the SN curve quantifying the fatigue strength of the un-notched material being designed, i.e. (Susmel & Taylor, 2007):

$$N_f = N_0\cdot\left(\frac{\Delta\sigma_0}{\Delta\sigma_{eff}}\right)^k \tag{5}$$

where $\Delta\sigma_0$ is the plain material endurance limit extrapolated at N_0 cycles to failure and k is the negative inverse slope of the plain material fatigue curve.

The formulation of the TCD reviewed above suggests that the number of cycles to failure can be estimated provided that a suitable recursive numerical procedure is used. This is due to the fact that while N_f is the unknown variable in the design problem, it is needed to estimate also the critical distance value from Eq. (1).

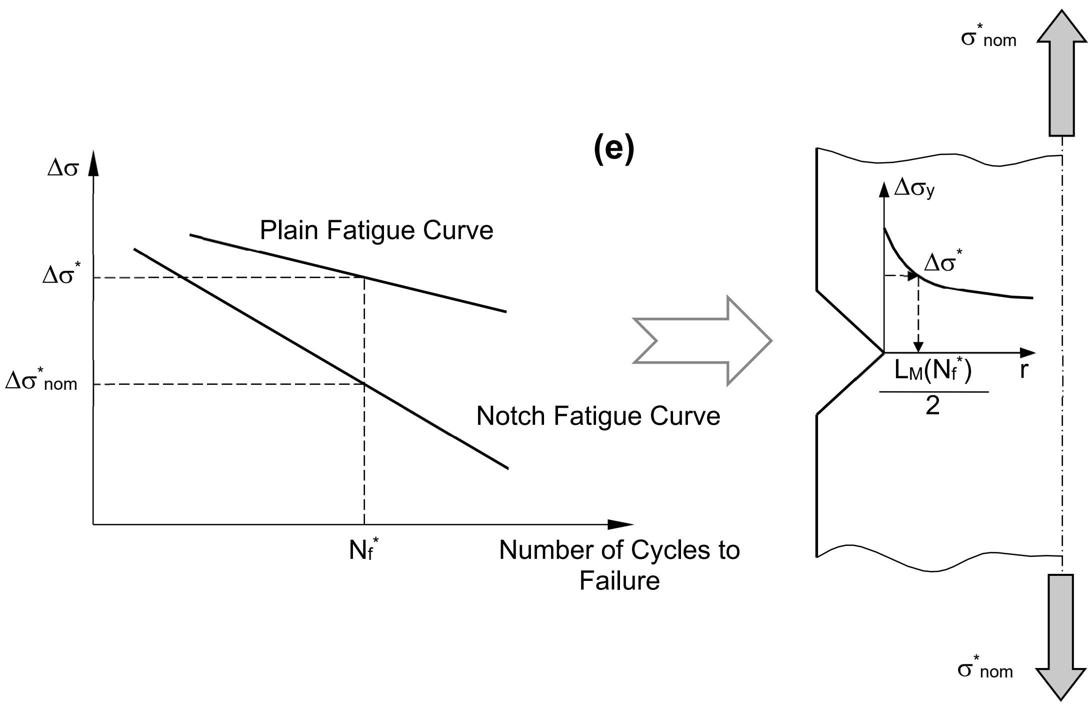

Fig. 2. Calibration of the L_M vs. N_f relationship by using two different fatigue curves.

Turning to the calibration of the L_M vs. N_f relationship according to definition (1), two different pieces of experimental information are obviously enough to estimate constants A and B. For instance, they could directly be derived from the critical distance determined under static loading and the critical distance estimated in the high-cycle fatigue regime (Susmel & Taylor, 2007). Unfortunately, this approach is not at all straight forward to be used in practice for the following two reasons (Susmel & Taylor, 2007; Susmel, 2009): (i) because the stress based approach is not accurate enough when it comes to modelling the behaviour of materials failing in the low-cycle fatigue regime; (ii) because the position of the knee point defining the endurance limit in the high-cycle fatigue regime is seen to vary as profile and sharpness of the calibration notches being tested change.

These two limitations can be overcome by simply determining constants A and B in Eq. (1) from the un-notched material fatigue curve and from another fatigue curve determined by testing specimens containing a notch having known profile and known sharpness (Susmel & Taylor, 2007; Susmel, 2009). This way of estimating constants A and B is explained through the SN diagram shown in Fig. 2. In particular, according to the Point Method's *modus operandi*, given a reference number of cycles to failure, N_f^*, it is straightforward to determine the distance from the notch tip, $L_M(N_f)/2$, at which $\Delta\sigma_y$ equals the value of the stress range that has to be applied to the plain material to break it at N_f^* cycles to failure (Fig. 2). According to this simple procedure, the critical distance value can then be determined for all the N_f values from the low- to the high-cycle fatigue regime, allowing constants A and B to be determined unambiguously. This simple strategy will be used in the next section to check whether the linear-elastic TCD is successful also in estimating fatigue lifetime of notched AM Ti6A14V in the as-manufactured condition.

3. Experimental details and summary of the results

A systematic experimental investigation was carried out by testing both plain and notched flat samples of AM Ti6Al4V containing three different geometrical features and having average thickness equal to 2.7 mm. The sharply V-notched samples had gross width, w_g, equal to 12.1 mm, net width, w_n, to 4.7 mm, root radius, r_n, to 0.4 mm and notch opening angle to 35°. These dimensions resulted in a net tensile stress concentration factor, K_t, of 3.37. The intermediate U-notched specimens had instead w_g =12.1 mm, w_n =5.8 mm, and r_n =0.7 mm (K_t =2.86); finally, the bluntly U-notched samples had w_g =12.1 mm, w_n =6.0 mm, and r_n =1.5 mm (K_t =2.10). The plain dog-bone specimens had gauge length width equal to 4.7 mm.

The parent material used for the present experimental investigation was AM Ti6Al4V. The specimens were manufactured using the DMLS technology via 3D-printer EOS M280 (with maximum laser power of 400 W). During manufacturing the laser power was set equal to 280 W, the scan speed to 1200 mm/sec and the hatch distance to 0.140mm. All the specimens were tested in the as-manufactured condition.

Table 1. Summary of the generated experimental results.

r_n *[mm]*	w_g *[mm]*	w_n *[mm]*	t *[mm]*	K_t	R	k	$\Delta\sigma_0$ or $\Delta\sigma_{0n}$ *[MPa]*	T_σ
-	4.6	4.6	2.7	1.00	-1	2.8	105.6	1.94
					0.1	3.3	114.1	1.98
1.5	12.1	6.0	2.7	2.10	-1	2.8	88.8	3.27
					0.1	3.7	104.2	3.54
0.7	12.1	5.8	2.7	2.86	-1	1.5	36.7	7.32
					0.1	4.8	107.1	2.21
0.4	12.1	4.7	2.7	3.37	-1	2.6	69.6	1.70
					0.1	3.9	84.6	1.83

The average mechanical properties of the titanium alloy DMLS-fabricated according to this procedure were as follows: Young's modulus equal to 110 GPa, ultimate tensile strength equal to 1413 MPa and Poisson's ratio to 0.33.

The fatigue tests were run by using a servo-hydraulic fatigue machine. Both the plain and the notched specimens were tested under sinusoidal axial loading, with the magnitude of the applied axial force being gathered continuously during testing through the axial loading cell. Since the net cross-sectional area of the specimens was very small, the fatigue tests were run up to the complete breakage of the samples themselves. All the experiments were run at a frequency of 10 Hz. The nominal load ratio, R, was set not only equal to -1, but also to 0.1, where the latter configuration was used to investigate the effect of superimposed static stresses on the overall fatigue strength of notched 3D-printed Ti6Al4V. The run-out tests were all stopped at $2 \cdot 10^6$ cycles to failure. All the tests were run at room temperature.

The results generated according to the experimental protocol described above are summarised in Table 1 in terms of negative inverse slope, k, endurance limit, $\Delta\sigma_0$ or $\Delta\sigma_{0n}$, extrapolated, for a probability of survival, P_S, equal to 50%, at $N_0=2 \cdot 10^6$ cycles to failure, and, finally, scatter ratio, T_σ, of the endurance limit for 90% and 10% probabilities of survival. This statistical post-processing was carried out by assuming a log-normal distribution of the number of cycles to failure for each stress level, with a confidence level equal to 95%.

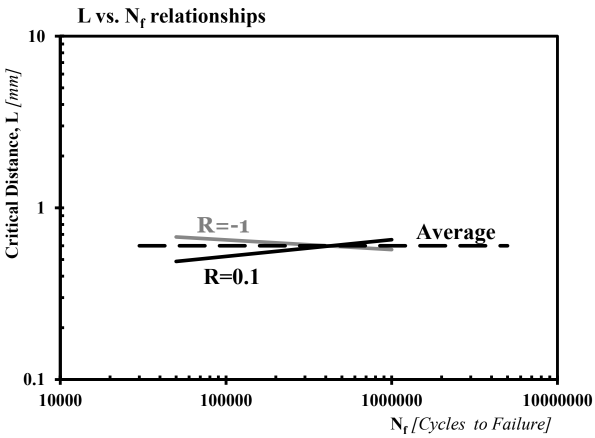

Fig. 3. Calibration of the L_M vs. N_f relationships for the AM titanium alloy under investigation.

4. Validation by experimental results

In order to apply the TCD to post-process the notch fatigue results summarised in Table 1, local stresses were determined using commercial FE software ANSYS®. The relevant linear-elastic stress fields in the notched specimens were determined by solving bi-dimensional FE models built by using 4-node structural plane elements (plane 182). According to the key hypothesis on which the formulation of the TCD is based, the numerical solutions were calculated by assuming that the AM titanium alloy under investigation behaves like a linear-elastic, homogeneous and isotropic material. Finally, in order to determine the required stress fields by systematically reaching an adequate level of numerical accuracy, the mesh density in the vicinity of the notch tips was gradually increased until convergence occurred.

According to the calibration strategy summarised in Fig. 2, constant A and B in Eq. (1) for the AM material being assessed were determined for P_S=50% from the experimental plain fatigue curve and the fatigue curve obtained by post-processing the results generated by testing the sharply notched specimens. This approach was used to determine the L_M vs. N_f relationship for both the R=-1 case and the R=0.1 case.

By post-processing the local-linear elastic stress field determined numerically for the sharply notched specimens, the procedure sketched in Fig. 2 applied by using the two calibration fatigue curves mentioned above returned the results shown in the chart of Fig. 3. This diagram makes it evident that the variation of L with N_f was very little. Accordingly, the hypothesis was formed that the critical distance could be taken constant and equal to its value averaged over the fatigue lifetime interval of interest. This approach was applied both to the R=-1 case and to the R=0.1 case, obtaining in both situations an average value of about 0.6 mm. Accordingly, the assumption was made that, for the specific AM material under investigation, constant B in Eq. (1) could be assumed to be invariably equal to zero, with the critical distance being as follows:

$$L = 0.6\,mm \tag{6}$$

This constant critical distance value was then used to post-process the experimental results being generated according to the Point, the Line and the Area Method. The obtained results are summarised in the experimental, N_f, vs. estimated, $N_{f,e}$, diagrams reported in Figs 4a to 4c (where the reported data are classified according to the sharpness of the notch). These charts make it evident that the predictions made using the LM (Fig. 4b) were uniformly distributed within the parent material scatter band. In contrast, the use of both the Point Method (Fig. 4a) and the Area Method (Fig. 4c) resulted in estimates characterised by a slight degree of conservatism, but mainly within the target error band.

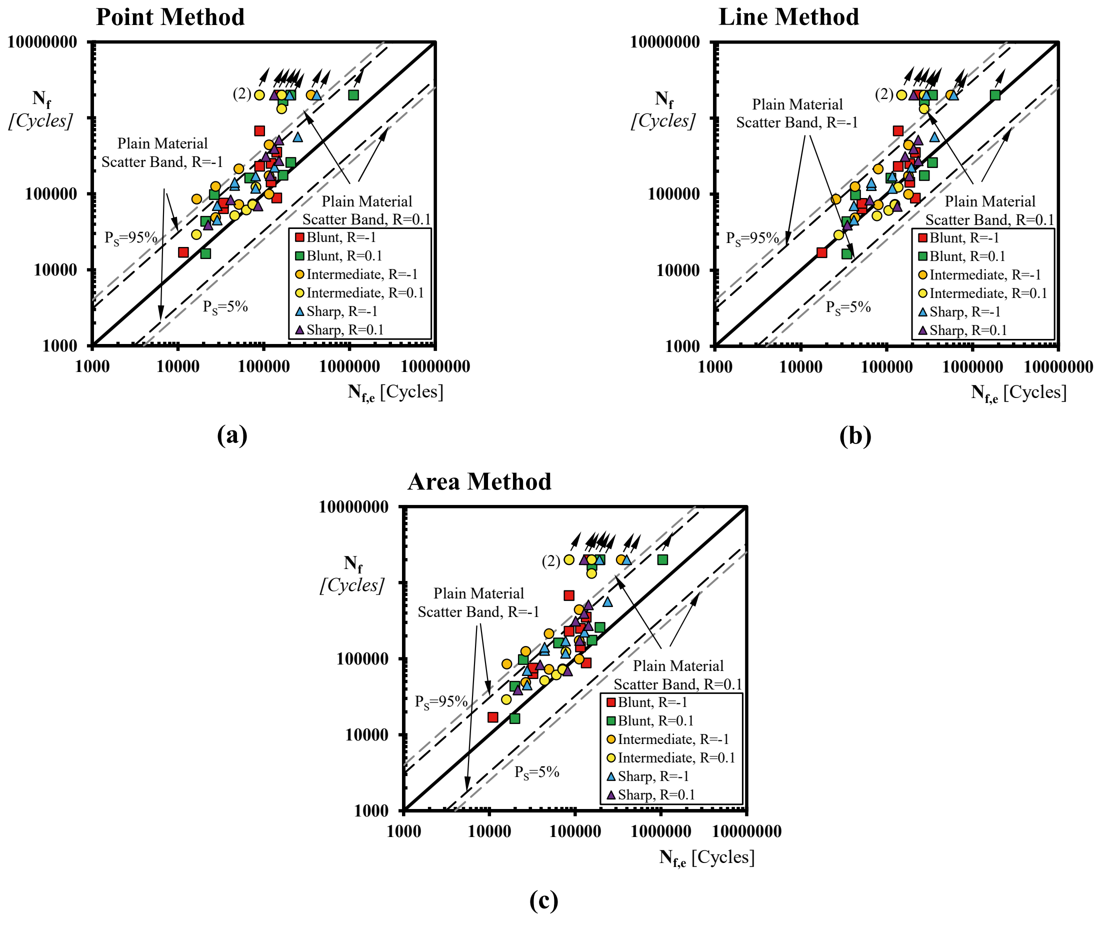

Fig. 4. Accuracy of the TCD in estimating the fatigue lifetime of the tested specimens of AM Ti6Al4V.

5. Conclusions

In the present investigation, a large number of specimens were tested to study the fatigue behaviour of AM Ti6Al4V weakened by notches having different sharpness. The notched samples used in the present investigation were tested in the Structures Laboratory of the University of Sheffield under fully-reversed axial loading (R=-1) as well as under a load ratio, R, equal to 0.1. The accuracy of the TCD in estimating fatigue lifetime of notched components of AM Ti6Al4V was checked against the fatigue results being generated.

According to the outcomes from this experimental/theoretical work, it is possible to conclude by observing that the TCD has proven to be remarkably accurate also in assessing notch fatigue strength of 3D-printed Ti6Al4V, with this holding true also when this material is used in the as-manufactured condition.

References

Chan, K.S., Koike, M., Mason, R.L., & Okabe, T., 2013. Fatigue life of titanium alloys fabricated by additive layer manufacturing techniques for dental implants. Metallurgical and Materials Transactions A 44(2), 1010-1022.

Herzog, D., Seyda, V., Wycisk, E., & Emmelmann, C., 2016. Additive manufacturing of metals. Acta Materialia 117, 371-392.

Neuber, H., 1958. Theory of notch stresses: principles for exact calculation of strength with reference to structural form and material. II Edition. Springer Verlag, Berlin, Germany.

Peterson R.E., 1959. Notch Sensitivity, *"Metal Fatigue"*. In: Sines G., Waisman J. L. (Ed.). McGraw Hill, New York, USA, pp. 293-306.

Qiu, C., Yue, S., Adkins, N.J., Ward, M., Hassanin, H., Lee, P.D., Withers, P.J., & Attallah, M.M., 2015. Influence of processing conditions on strut structure and compressive properties of cellular lattice structures fabricated by selective laser melting. Materials Science and Engineering: A 628, 188-197.

Razavi, S.M.J., Van Hooreweder, B., Berto, F., 2020. Effect of build thickness and geometry on quasi-static and fatigue behavior of Ti-6Al-4V produced by Electron Beam Melting. Additive Manufacturing 36, 101426.

Susmel, L., 2009. Multiaxial Notch Fatigue: from nominal to local stress-strain quantities. Woodhead-CRC-Elsevier, Cambridge, UK.

Susmel L. Taylor, D., 2007. A novel formulation of the Theory of Critical Distances to estimate Lifetime of Notched Components in the Medium-Cycle Fatigue Regime. Fatigue and Fracture of Engineering Materials and Structures 30(7), 567-581.

Tanaka, K., 1983. Engineering formulae for fatigue strength reduction due to crack-like notches. International Journal of Fracture 22, R39-R45.

Taylor , D., 1999. Geometrical effects in fatigue: a unifying theoretical model. International Journal of Fatigue 21, 413-420

Taylor, D., 2007. The Theory of Critical Distances: A new perspective in fracture mechanics. Elsevier, Oxford, UK

Sheppard, S.D., 1991. Field effects in fatigue crack initiation: long life fatigue strength. ASME Journal of Mechanical Design 113, 188-194.

Bellett, D., Taylor, D., Marco, S., Mazzeo, E., Guillois, J., Pircher, T., 2005. The fatigue behaviour of three-dimensional stress concentrations. International Journal of Fatigue 27, 207-221.